

# Diffusion bonding of gray cast iron and AISI 1040 couple

C. CARBOGA\*

*Nevsehir University, Faculty of Engineering and Architecture, Material Engineering Department, Nevsehir, Turkey*

In the present study, gray cast iron was diffusion bonded to medium carbon steel. The effect of bonding temperature and holding time at the reached temperature on the microstructural developments across the joint region were investigated. After diffusion bonding, microstructural analysis including metallographic examination, energy dispersive spectrograph (EDS), microhardness measurement and shear strength were investigated. From the results, it was seen that bonding temperature and holding time were effective on the Si and C diffusion from gray cast iron to AISI 1040 steel that affected the microstructure. The microstructure of interface region changed from ferrite to pearlite by increasing temperature and holding time. It was also seen that bonding temperature and holding time were effective on the microstructure, microhardness and shear strength of the joints.

(Received August 23, 2013; accepted March 13, 2014)

*Keywords:* Diffusion bonding, AISI 1040, Gray cast iron

## 1. Introduction

Diffusion bonding is only one of the many solid-state joining processes where in joining is accomplished without the need for a liquid interface or melting and resolidification. In this bonding process in which two materials, similar or dissimilar, can be bonded in solid state [1]. The main advantages of this joining technique is the lack of structural discontinuity across the interface at high temperature and pressure [2]. Coalescence of the faying surfaces is accomplished through the application of pressure at elevated temperature. No melting and only limited macroscopic deformation or relative motion of the parts occurs during welding. Diffusion bonding is particularly well suited for joining many dissimilar metal combinations, especially when the melting points of two metals differ widely or when the materials are not metallurgically compatible [3]. Fusion welding for dissimilar materials combinations stress development at interface also occurs owing to their difference in coefficient of linear expansion and this leads to formation of micro-cracks at the bonded region [4]. For these reasons, diffusion bonding does not involve melting or gross macroscopic interface distortion, the microstructure of the bond region is similar to that of regions remote from the join and has parent metal properties [5].

Cast iron is widely used for structural components because casting has a great advantage that the cast iron products can be produced in near-net-shape [6–7]. Most of the welding performed on cast iron is repair welding [8]. But, recently a few study with fusion welding, diffusion bonding and liquid-solid casting studies performed between cast iron and steel for a new metal couple [6–10]. However, cast iron is known as a hardly welding material. The poor weldability of cast iron can be attributed to two factors, the formation of martensite in the heat affected zone (HAZ), and the development of hard, brittle iron carbide in the zone of partial fusion [11–12]. Thus;

diffusion bonding seems to be a proper method for joining these materials.

In the present study, diffusion bonding method has been chosen for joining the gray cast iron and medium carbon steel. The reason for choosing is to determine the weldability of brittle properties of gray cast iron and hardenability properties of medium carbon steel couple. For this aim, gray cast iron and medium carbon steel couple were diffusion bonded. The effects of bonding temperature and holding time on the microstructure, hardness and shear strength of the joint were investigated.

## 2. Materials and method

In this study, a gray cast iron (with 3.2 C % and 2 % Si) and AISI 1040 type medium carbon steel (with 0.42 C %, 0.7 Mn % and 0.2 Si %) were used for diffusion bonded. Gray cast iron specimens were obtained from the rods that were casted in diameter  $\phi 50 \times 400$  mm. The AISI 1040 steel was provided from a set material having 10 mm thickness. For diffusion bonding, specimens were cut into  $10 \times 10 \times 10$  mm dimension from these materials using sensitive specimen cutting machine. Prior to diffusion bonding, one face of each specimen was processed in order to achieve a predetermined degree of roughness using 1200 mesh grind paper. The samples were then degreased in an ultrasonic bath using acetone.

Diffusion bonding was made in an argon atmosphere in the bonding chamber of the induction heating unite designed for diffusion bonding. The diffusion bonding couples were heated to bonding temperature with the heating rate of  $40 \text{ }^\circ\text{C min}^{-1}$ . The bonds made under the pressure of 8 MPa at four different temperatures, 850, 900, 950 and 1000  $^\circ\text{C}$ . For each temperature two different holding times, 15 and 30 minutes were used.

Table 1. Bonding conditions.

Specimen	Bonding temperature (°C)	Bonding time (minute)
1	850	15
2	850	30
3	900	15
4	900	30
5	950	15
6	950	30
7	1000	15
8	1000	30

The bonding conditions are given in Table 1. Once the bonding process was completed and the samples were slowly cooled at the rate of 5 °C/min. to room temperature before removal from the chamber in order to prevent cracking.

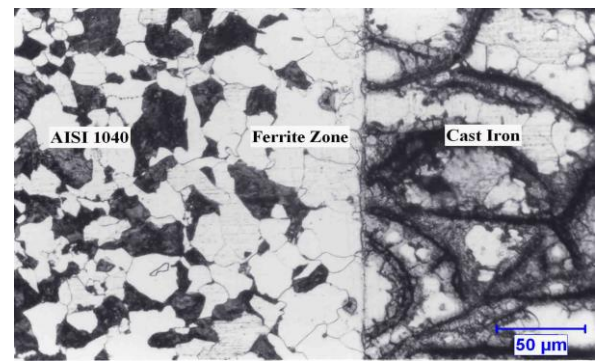
After bonding, the bonded specimens were cut transversely through the bond and metallographically polished to 3 µm diamond finish for metallographic examination. For microstructural examination, diffusion bonded couple was etched with 2 % nital. Metallographic observations were performed by optic and SEM microscopies and changes in the interface region were investigated energy dispersive spectroscopy (EDS).

The bonds were mechanically tested using a shear test apparatus. The bonded specimens were further machined to produce shear test specimens with dimensions 8x8x10 mm, to eliminate edge effects on test data. An Instron tensile testing machine set at a crosshead speed of 0.5 mm. min<sup>-1</sup> was used for the shear tests. The microhardness values were measured on both sides of the bonded specimens using a 15 g load.

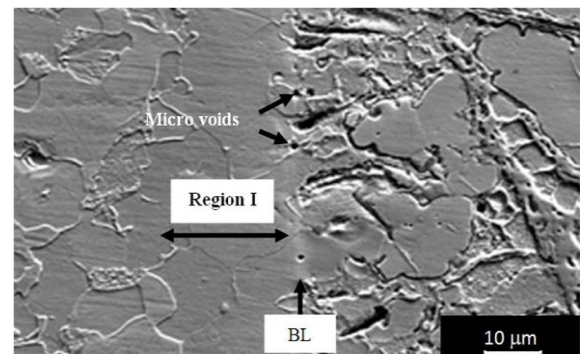
### 3. Results and discussion

#### 3.1 Microstructure

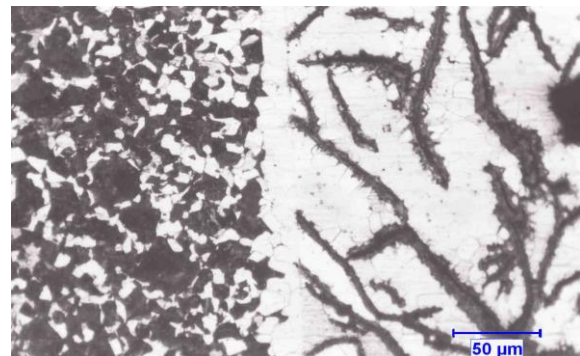
The micrographs for the specimens bonded at 850, 900, 950 and 1000 °C for 15 and 30 minute are shown in Figs. 1-4.



(a)



(b)

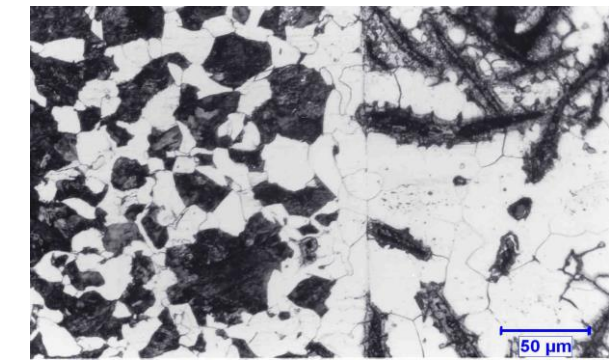


(c)

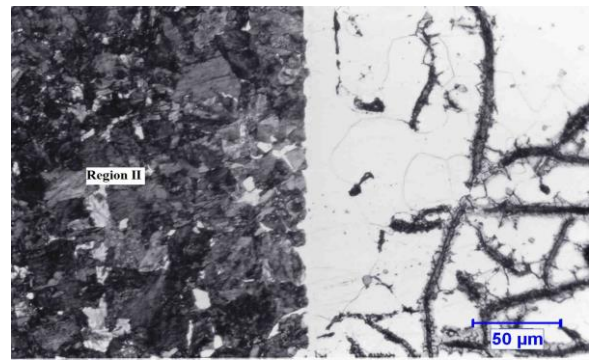
Fig. 1. Optic (a) and SEM (b) micrographs of the specimens bonded at 850°C for 15 and optic micrograph (c) at 850°C for 30 minutes (BL: bond line).

From the Fig. 1a, interface line between bonded specimens at the 850 °C for 15 minute clearly seen. This line was occurred from a lot of microvoid along the interface according to the low temperature and time (clearly seen in Fig. 1b). other specimens exhibited a good bonding along the interface. From the figures, it can be seen that different microstructural regions occurred at the bond area depending on the bonding temperature. Therefore, the bond area was divided into three different regions to explain the mechanism of the microstructural formation.

Region I: This region at the side of AISI 1040 steel and close to bond line was composed of fully ferrite for bonding temperatures of 850 and 900 °C and pearlite for bonding temperatures of 950 and 1000 °C (Figs. 1 - 4).



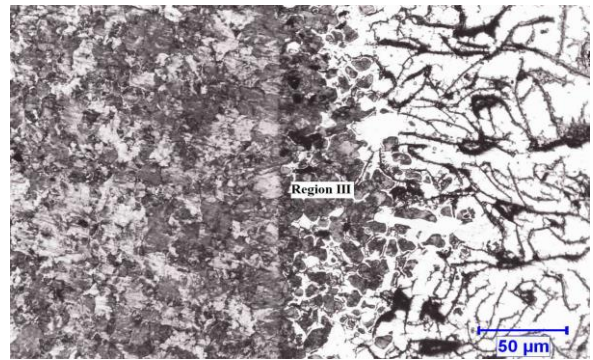
(a)



(a)

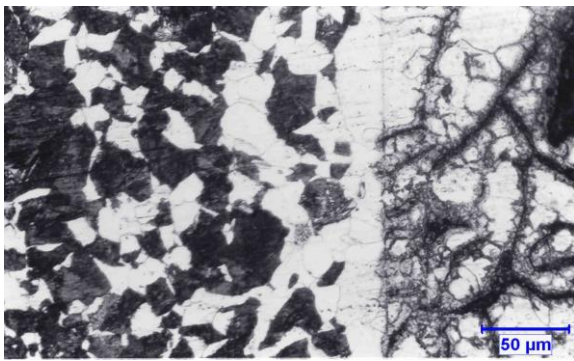


(b)

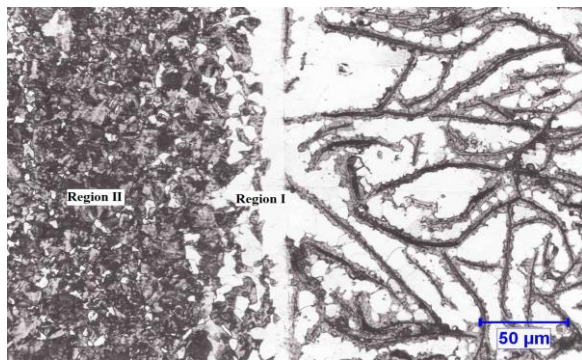


(b)

Fig. 2. Optic micrographs of the specimens bonded at 900°C for 15 (a) and 30 (b) minutes.

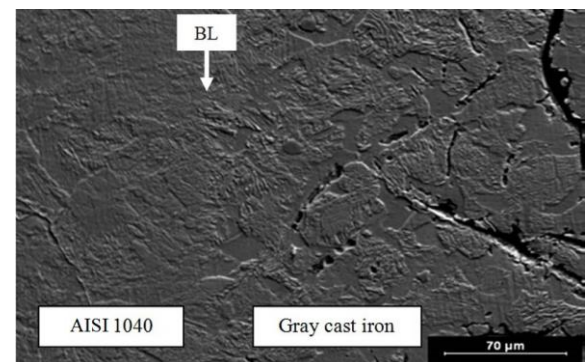


(a)



(b)

Fig. 3. Optic micrographs of the specimens bonded at 950°C for 15 (a) and 30 (b) minutes.



(c)

Fig. 4. Optic micrographs of the specimens bonded at 1000°C for 15 (a) and 30 (b) minutes and SEM (c) micrograph of the bond interface of the specimens bonded at 1000 °C for 30 minute (BL, bond line; P, pearlite; F, ferrite).

Table 2. Ferrite and pearlite occurrence distance in interface region.

Specimen No	Ferrite distance (µm)	Pearlite distance (µm)
1	45	-
2	20	75
3	25	50
4	12	150
5	23	100
6	-	175
7	5	125
8	-	210

The width of this region is shown in Table 2. As can be seen from this table, as the bonding temperature increased, the width of this region decreased and disappeared after 900 °C. It is thought that Si diffusion from gray cast iron side is effective on the formation of ferrite in region I. It is well known that Si element in steel has an important effect on ferrite formation promoting graphitization [13]. However, as the bonding temperature was increased the formation of pearlite was seen in region I although Si content increased slightly (Fig. 5).

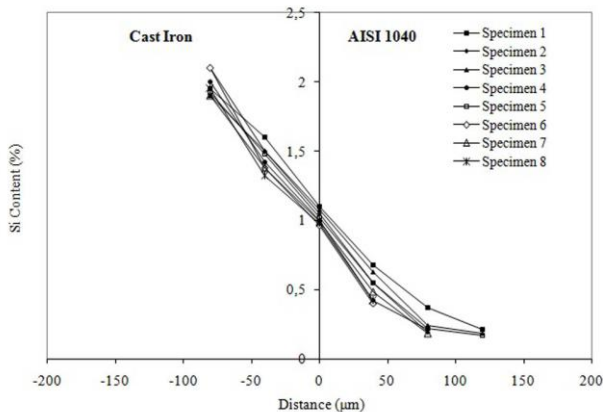


Fig. 5. Silicon concentration profiles in interface region from EDS results.

This also shows that carbon content diffused from gray cast iron side to AISI 1040 steel is important on the formation of pearlite in region I at the bonding temperatures of 950 and 1000 °C. It is thought that austenite grains in regions I and II were not saturated with carbon since the content of carbon diffused from gray iron side was low because of lower dissolution of graphite flakes at 850 and 900 °C. During the cooling from 850 and 900 °C the carbon element in region I coming from gray iron diffused towards region II because of Si diffusion from gray iron side [13]. However, as the bonding temperature was increased to 950 and 1000 °C the content of carbon diffused from gray iron side increased. This also means that austenite grains at regions I and II were supersaturated by carbon at the bonding temperatures of 950 and 1000 °C. Although Si contents were slightly higher at bonding temperatures of 950 and 1000 °C than those of 850 and 900 °C, ferrite formation were not seen at the region I for higher bonding temperatures. This can also be related to the saturated austenite grains in region II.

Region II: This region, between unaffected parent metal of AISI 1040 steel and region I, was mainly composed of ferrite plus pearlite for lower bonding temperatures (850 and 900 °C, Figs. 1 and 2) and pearlite for higher bonding temperatures (950 and 1000 °C, Figs. 3 and 4).

Table 3. Ferrite and pearlite concentrations in the II. region.

Specimen No	Ferrite (%)	Pearlite (%)
1	78	22
2	28	72
3	50	50
4	12	88
5	40	60
6	-	100
7	30	70
8	-	100

Table 3 shows the volume fractions of pearlite and ferrite in this region. As can be seen from the table, as the bonding temperature increased pearlite content increased. It can also be seen from the Table 2 that the width of region II increased with the increase in bonding temperature. As the bonding temperature and time increased the carbon dissolution from the graphite flakes increased. Therefore the diffusion of carbon from gray cast iron side towards AISI 1040 steel increased, and this caused an increase in the amount of pearlite. For the specimens bonded at 950 °C the region II was mainly composed of pearlite, while the specimens bonded at 1000 °C the region II consisted of fully pearlite.

Region III: In this region at the gray cast iron side (Fig. 4), depending on the bonding temperature and time, the microstructure was change from ferrite plus graphite flakes to ferrite plus pearlite. As the bonding temperature increased dissolution of graphite flakes increased. Also, the diffusion of C and Si from gray cast iron side towards AISI 1040 steel increased (Fig. 5). Therefore, the pearlite plus ferrite formation took place at the gray cast iron side near bond line where carbon was not as high as to produce graphite. Therefore it can be said that the area near bond line at the side of gray cast iron (region III) became a carbon steel for a bonding temperature of 1000 °C.

### 3.2 Hardness

The microhardness measurements taken across the bond region for the bonded specimens are shown in Fig. 6.

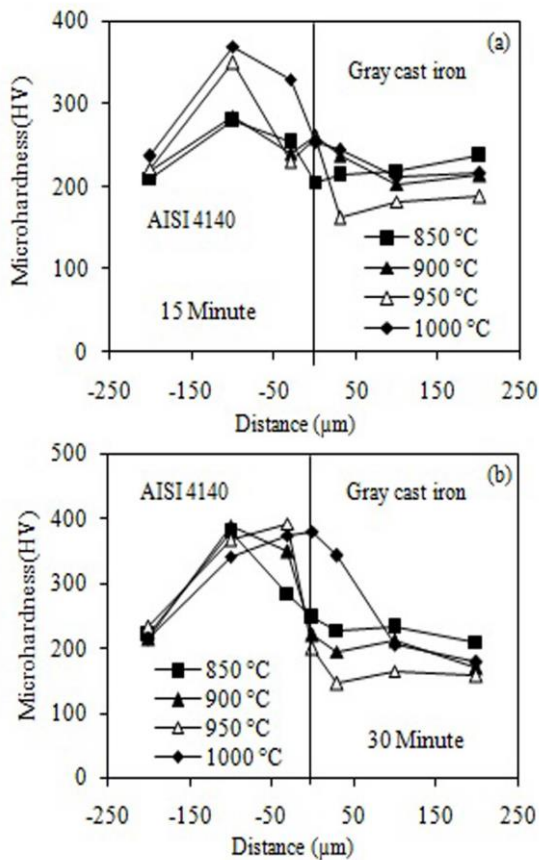


Fig. 6. Microhardness distribution in interface region.

As can be seen from the figure, the hardness values first increased in the region II and decreased in region I for the specimens bonded at 850 °C and 900 °C, respectively. For these specimens hardness values were also lower on the bond line because of the formation of ferrite. The increase in hardness in region II was related to the pearlite in the microstructure, while lower hardness values in region I was associated with the ferritic microstructure for the specimens bonded at 850 and 900 °C (Figs. 1 and 2). For the specimen bonded at 950 °C, the increase in hardness started at the region II and continued up to bond line because of the pearlitic microstructure. For the specimens bonded at 1000 °C the hardness increase started at region II and continued up to gray cast iron side because of the formation of pearlite (Fig. 4)

From the results of hardness measurement, it can be concluded that hardness increases as the bonding temperature increases. This was related to the graphite dissolution and carbon diffusion that increased the volume fraction of pearlite (Table 3).

### 3.3 Shear strength

The bond shear strength as a function of temperature and time are shown in Fig. 7.

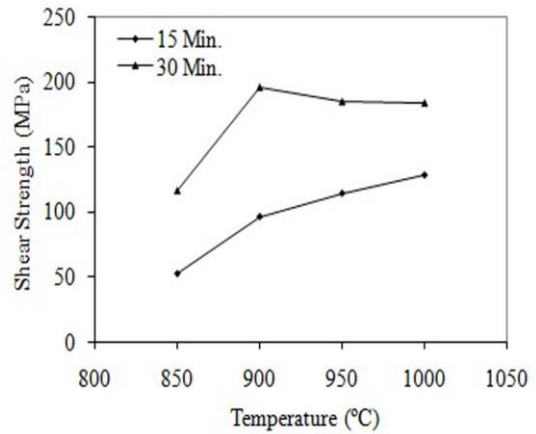


Fig. 7. Compressive shear strength of bonds in as a function of bonding temperatures and times.

As can be seen from the figure, higher shear strength values were obtained for higher bonding temperature and longer bonding times. Because, lamellar graphite structure in side of cast iron of the interface has evolved into pearlitic structure. All joints were failed at the gray iron side and this can be seen on the fracture surfaces shown in Figs. 1-4. This can be related to the graphite lamella where stress concentration was much more.

Although all joints were failed at the gray cast iron side, it was observed some differences on the fracture surfaces. Since higher dissolution of graphite flakes at the bonding temperature of 1000 °C near bond line, graphite flakes have not been detected as much as other bonding temperatures.

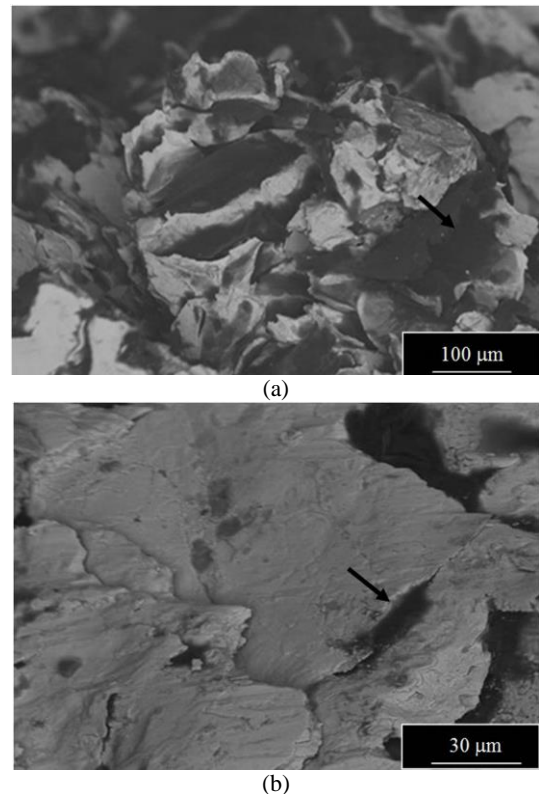


Fig. 8. SEM images of fracture surfaces of the bonds made at a) 850 °C and b) 1000 °C (arrow shows graphite flake).

This can be seen clearly on the fracture surfaces as shown for the specimens bonded at 850 °C and 1000 °C in Figs. 8a and b, respectively.

#### 4. Conclusions

The effects of bonding temperatures and times on the interface microstructure and shear strength of diffusion bonded gray cast iron and AISI 4140 steel were investigated.

- The width of region II increased up to bonding temperature of 950 °C, but the width of region I decreased.
- For bonding temperature of 1000 °C, region I dissipated and microstructure became fully pearlite.
- For bonding temperature of 1000 °C, pearlite formation was seen at the gray cast iron and this region became steel.
- Hardness values at the bonding area increased.
- Shear strength increased with increasing bonding temperature and time.

#### References

- [1] M. W. Mahoney, C. C. Bampton, *ASM Metals Handbook*, **6**, 514 (1993).
- [2] L. I. Duarte, F. Viana, A. S. Ramos, M. T. Vieira, C. Leinenbach, U. E. Klotzand, M. F. Vieira, *Journal of Alloys and Compounds*, **536**, 424 (2012).
- [3] M. M. Schwartz, D. F. Paulonis, *Welding handbook*, **3**, 311 (1980).
- [4] M. Ghosh, S. Chatterjee, B. Mishra, *Materials Science and Engineering A* **363**, 268 (2003).
- [5] M. F. Islam, N. Ridley, *Scripta Materialia*, **38**, 1187 (1998).
- [6] M. Hatate, T. Shiota, N. Abe, M. Amano, T. Tanaka, *Vacuum*, **73**, 667 (2004).
- [7] K. Matsugi, M. Konishi, O. Yanagisawa, M. Kiritani, *Journal of Materials Processing Technology*, **150**, 300 (2004).
- [8] B. Xiong, C. Cai, B. Lu, *Journal of Alloys and Compounds*, **509**(23), 6700 (2011).
- [9] S. Kolukisa, *Journal of Materials Processing Technology*, **186**, 33 (2007).
- [10] B. Kurt, N. Orhan, A. Haşçalık, *Materials & Design*, **28**, 2229 (2007).
- [11] E. M. El-Banna, M. S. Nageda, M. M. A. El-Saadat, *Materials Letters*, **42**, 311 (2000).
- [12] E. M. El-Banna, *Materials Letters*, **41**, 20 (1999).
- [13] E. C. Bain, H. W. Paxton, *Alloying elements in steel*, Metals Park, OH, American Society for Metals, (1996).

\*Corresponding author: ccarboga@gmail.com